Remote Sensing of Environment 268 (2022) 112777

Contents lists available at ScienceDirect

Remote Sensing of Environment

journal homepage: www.elsevier.com/locate/rse

Large wildfire driven increases in nighttime fire activity observed across CONUS from 2003–2020

Patrick H. Freeborn [a,*], W. Matt Jolly [a], Mark A. Cochrane [b], Gareth Roberts [c]

[a] US Forest Service, Rocky Mountain Research Station, Fire Sciences Laboratory, 5775 Highway 10 West, Missoula 59803, MT, USA
[b] Appalachian Laboratory, University of Maryland Center for Environmental Science, 301 Braddock Road, Frostburg 21532, MD, USA
[c] Geography and Environmental Science, University of Southampton, Building 44, University Road, Southampton SO17 1BJ, UK

ARTICLE INFO

Edited by Dr Marie Weiss

Keywords:
Nighttime fire activity
Nighttime persistence
Nighttime proportion
Large wildfires

ABSTRACT

Despite the ecological and socioeconomic impacts of wildfires, little attention has been paid to the spatiotemporal patterns of nighttime fire activity across the conterminous United States (CONUS). Daytime fire radiative power (FRP) detected by the Moderate Resolution Imaging Spectroradiometer (MODIS) was nearly evenly split (54% vs. 46%) between inside and outside wildfires from 2003 to 2020. In contrast, 94% of nighttime FRP was detected within wildfires, of which 95% was detected within large wildfires (> 2023 ha). Nighttime proportions (i.e., the proportion of total summed FRP detected by MODIS at night) were lowest (3%) outside wildfires when coincident 1000-hr fuel moistures were highest and vegetation fires were smaller and less intense. As 1000-hr fuel moistures decreased, MODIS active fire pixels shifted out of agricultural and prescribed fires and into wildfires with higher nighttime per-pixel values of FRP such that nighttime proportions peaked at 29% for the largest wildfires. Increases in nighttime proportions within larger wildfires were attributed to increases in nighttime persistence whereby under the driest conditions, daytime fire activity detected by MODIS was more likely to continue burning with sufficient vigour to be detected again at night. From 2003–2020, MODIS detected significant ($p < 0.01$) increasing trends in nighttime wildfire fire activity, with a +54%, +42% and +21% increase in the annual nighttime sum of FRP, annual nighttime active fire pixel counts and annual mean nighttime per-pixel values of FRP, respectively, detected in the latter half of the study period. Nighttime trends were corroborated using observations from the Visible Infrared Imaging Radiometer Suite (VIIRS) as well annual wildfire statistics reported by U.S. federal, state and local agencies. Moreover, MODIS detected a significant positive trend in the nighttime proportion of FRP emitted from wildfires, indicating that in the absence of diurnal differences in detection biases, increases in nighttime fire activity since 2003 have outpaced daytime increases. However an analysis of MODIS omission rates revealed that increasing nighttime proportions were at least partially attributed to a relatively greater improvement in nighttime detection performance compared to the daytime for larger wildfires burning during drier conditions. Nighttime fire activity already poses additional risks to firefighters and communities, and this work suggests that projected increases in the frequency of large wildfires will be accompanied by increases in the extent and intensity of nighttime fire activity.

1. Introduction

Vegetation fires are a common global disturbance that shape ecosystem patterns and processes, influence terrestrial and atmospheric carbon balances, control vegetation structure and distribution and modify land surface-atmosphere coupling (Bowman et al., 2009). Compared to other vegetation fire types, such as agricultural fires and prescribed fires, wildfires in the United States (US) are uniquely classified because they are unplanned (Gill et al., 2013), either through natural, unintentional or malicious ignitions, and are therefore assigned firefighting resources to implement a range of suppression strategies (Hand et al., 2017; Riley et al., 2018). The conterminous US (CONUS) currently resides on the leading edge of an increasing trend in wildfire burned area (NICC, 2021), and particularly large wildfires (Stephens, 2005; Littell et al., 2009; Dennison et al., 2014), that drives suppression costs (Abt et al., 2009), threatens property loss (Syphard et al., 2012) and compromises firefighter and public health and safety (Cova, 2005; Withen, 2015; Roberts and Wooster, 2021).

* Corresponding author.
E-mail address: patrick.h.freeborn@usda.gov (P.H. Freeborn).

https://doi.org/10.1016/j.rse.2021.112777
Received 25 June 2021; Received in revised form 22 October 2021; Accepted 25 October 2021
Available online 10 November 2021

The area burned by wildfires can be reduced to the product of two terms: duration and spread rate. Since most studies have concentrated on the annual area burned by wildfires within large regions, examinations of wildfire duration have mainly focused on season length. The fire activity season length (FASL), or the number of days per year when fires are actively burning, is increasing across CONUS (Freeborn et al., 2016). Expansions of the FASL coincide with expansions of the fire weather season length (FWSL), or the number of days per year when weather conditions are most conducive to the ignition and spread of wildland fires (Jolly et al., 2015). Expansions in both the FASL and FWSL have led to an increase in the number of days per year that wildfires are being managed, as evidenced by an increase in the number of days between wildfire discovery and control dates (Westerling et al., 2006). Although the seasonal duration of regional wildfire activity (i.e., months) is the culmination of multiple, temporally overlapping wildfire events burning at shorter time scales, the factors affecting individual incident lifetimes (i.e., days to weeks) or the length of the diurnal burning period during which fires spread most rapidly, typically sometime between 1000 and sundown (i.e. hours), have largely remained unexplored.

In contrast to duration which covers a broad range of temporal scales, fire growth rates are more appropriately interpreted at the shortest time scales (i.e., hourly to daily). Weather variables such as wind speed facilitate fire spread and intensity by improved heat transfer to adjacent fuels and by providing oxygen for combustion. Other weather factors, such as temperature, humidity and solar insolation, can indirectly affect wildfire spread rates through their influence on fuel moisture content (Viney, 1991). Fuel moisture content variations are the dominant factor in determining whether or not new wildfires will start (Chuvieco et al., 2004), and in the absence of wind, fuel moisture content strongly drives wildfire spread rates (Rossa, 2017). Given that fire weather conditions vary over 24-hr periods, they can potentially have strong impacts on diurnal variations in fuel moisture content and subsequent fire activity (Williamson et al., 2016). However very few studies have focused on characterizing diurnal variations in fire activity. Williamson et al. (2016) showed that the occurrence of nighttime burning across Australia was greatest during periods of the highest fire danger. However, this study did not characterize seasonal differences in daytime and nighttime fuel moisture nor did it leverage additional information about fire size and intensity.

Despite the complicated ecological and socioeconomic trade offs associated with wildfires (Moritz et al., 2014), little attention has been paid to nighttime fire activity across CONUS (Little, 2020). Periods of low fire behaviour during the nighttime hours provide firefighters with opportunities to rehydrate, eat, sleep and lower their core body temperatures (Aisbett et al., 2012; Larsen et al., 2015; Vincent et al., 2018). However, if wildfires do not subside at night, even fire camps may not offer respite in the face of increasing nighttime smoke production (McNamara et al., 2012). Working at night is not uncommon on large wildfires (Graham, 2003). Whilst cooler temperatures and higher relative humidities may enable firefighters to make better progress, nighttime operations take on additional risk due to reduced visibility. Vehicle accidents were the second leading cause of wildland firefighter fatalities from 1990 to 2006, and although the times of the accidents were not reported, the possible effect of darkness and/or fatigue was not discounted (Mangan, 2007). Without accounting for the number of firefighters or the number of hours worked on night shifts, Britton et al. (2013) reported that 28.8% of slips, trips and falls and 20.9% of equipment/tools/machinery injuries experienced by US department of Interior (DOI) wildland firefighters occurred at night. The dangers of unseen hazards such as snags (Dunn et al., 2019) and rolling debris are ever present, but may be compounded if a firefighter is injured at night when they are more difficult to access, treat and extricate.

Extreme fire behaviour is possible at night under the driest and windiest conditions. Firefighters rely on the ability to recognize changing fire environments to avoid entrapments (Page et al., 2019), and without the ability to see the motion of the clouds or the smoke plume, firefighter safety can be compromised during extreme nighttime burning conditions when there are rapid, unexpected changes in fire behavior. While rare, firefighter entrapments have occurred at night (Page et al., 2019; Bagley and Clements, 2021). To avoid these situations, firefighters will completely disengage from the fire and may be reassigned to help emergency service personnel warn and evacuate communities - an inherently more complicated situation at night as evidenced by the Chimney Tops 2 fire in Gatlinburg, TN, in 2016 (Kuligowski et al., 2020). Compared to the day when most people are at work or in school, people return to their homes at night. Hence emergency services must have access to accurate census data and addresses (Bhaduri et al., 2007; Li et al., 2019) when evacuating residential populations during extreme nighttime wildfire events since people may wait for official information before making their own decision to evacuate when it's dark (Wong et al., 2020).

Ultimately, the annual area burned by wildfires across CONUS is the result of multiple, individual fires burning at different spread rates and intensities through the day and night. As such, more work is needed to characterize the diurnal cycle of wildfires and its drivers. In this study, we intersect an 18 year time series (2003–2020) of daytime and nighttime Moderate Resolution Imaging Spectroradiometer (MODIS) active fire detections across CONUS with a historical database of wildfire perimeters to differentiate diurnal fire cycles inside and outside of wildfires. Furthermore, we use a moderate resolution surface weather dataset to explore and characterize seasonal differences in the prevalence of wildfires as well as the influence of fuel moisture variations on observed fire radiative power (FRP), nighttime persistence, and MODIS daytime and nighttime detection performance. Finally, we analyse trends in nighttime fire activity detected by MODIS and corroborate these trends using observations from the Visible Infrared Imaging Radiometer Suite (VIIRS) and US Government interagency wildfire statistics.

2. Methods

2.1. Data

Diurnal fire activity across CONUS from 2003 to 2020 was characterized using the Standard MODIS Version 6 Terra and Aqua active fire (AF) products (Giglio et al., 2016) obtained from the Fire Information for Resource Management System, FIRMS (Davies et al., 2009). Relevant attributes for each MODIS 1km AF pixel included latitude and longitude, date and time, satellite, day/night flag, Fire Radiative Power (FRP), along-scan pixel size, inferred hotspot type and detection confidence. All AF pixels labelled as "presumed vegetation fires" were retained regardless of detection confidence. Combinations of the satellite and day/night flag were used to distinguish the four daily MODIS overpasses that occur approximately at 0130, 1030, 1330 and 2230 local time. From 20 January 2012 to 2020, the MODIS AF products were supplemented with the Visible Infrared Imaging Radiometer Suite (VIIRS) AF products generated from the Suomi National Polar-orbiting Partnership (S-NPP) satellite (Schroeder et al., 2014). S-NPP VIIRS has 375m spatial resolution and provides two daily overpasses approximately at 0130 and 1330 local time. The Standard VIIRS Version 1 active fire products obtained from FIRMS contained the same AF pixel attributes as MODIS and were similarly processed.

Different vegetation fire types are distinguished from each other by the fuels in which they burn, how and why they were ignited, how they were managed, and their final size. Unplanned wildfires that typically garnered a suppression response were distinguished from other vegetation fire types by intersecting AF pixels with wildfire perimeters $\geq$405 ha in western CONUS and $\geq$202 ha in eastern CONUS compiled between 2003–2018 by the Monitoring Trends in Burn Severity (MTBS) project (Eidenshink et al., 2007). To capture smaller wildfires and extend the temporal coverage, AF pixels from 2003–2020 were also intersected with incident perimeters created via the National Wildfire Coordinating

Group (NWCG) Standards for Geospatial Operations (NWCG, 2021) and obtained from the National Incident Feature Services (NIFS, 2021). All AF pixels were buffered by 1/2 their along-scan pixel size to account for increasing pixel sizes with scan angle and geolocation accuracy. At the very least, AF pixels were temporally clipped to the year in which the wildfire occurred. Where possible AF pixels were restricted to discovery and contain dates obtained by matching MTBS and NIFS perimeters with records in the Fire Program Analysis Fire Occurrence Database, FPA FOD (Short, 2014). Each AF pixel detected inside a wildfire perimeter was assigned a fire size class defined by the NWCG, as follows: A & B $<$ 4 ha; 4 ha $\leq$ C $<$ 40 ha; 40 ha $\leq$ D $<$ 121 ha; 121 ha $\leq$ E $<$ 405 ha; 405 ha $\leq$ F $<$ 2023 ha; 2023 ha $\leq$ G. Note that NWCG size classes refer to the final burned area and not the instantaneous area of flaming and smoldering combustion.

Active fire pixels detected outside of a MTBS or NIFS wildfire perimeter were not assigned a specific fire type and are generically referred to as "outside wildfires" or "other" vegetation fire types (Randerson et al., 2012). The majority of "other" fire types were likely agricultural fires used to remove crop residue (McCarty et al., 2007, 2009) or prescribed fires used for ecosystem restoration (Ryan et al., 2013) or fuel hazard reduction (Stephens et al., 2012). As reported by Lin et al. (2014), it is possible - if not expected - that some AF pixels assigned to "other" fire types may in fact be associated with wildfires that were not included in the MTBS or NIFS datasets either because they were smaller than the MTBS minimum mapping threshold or the incident perimeter was never uploaded to the NIFS.

The near-surface environment coincident with each AF pixel was characterized using gridMET - a daily, gridded meteorological dataset covering CONUS from 1979 to 2019 (Abatzoglou, 2013). Following Jolly et al. (2019), the 1978 version of the National Fire Danger Rating System (Bradshaw et al., 1984; Cohen and Deeming, 1985) was used to generate a daily, CONUS-wide 4 km gridded climatology of fuel moistures. Large fuel particles with diameters ranging from 7.6 to 20.3 cm are referred to as "1000-hr" fuels (Fosberg et al., 1981) and their fuel moistures were calculated using the daily maximum temperature and minimum relative humidity. Large fuels respond slowly to changes in atmospheric moisture and are therefore most suitable for capturing the low-frequency seasonality of moisture conditions. In locations such as grasslands and agricultural fields where coarse woody debris is sparse or absent, the 1000-hr fuel moisture is more indicative of the near-surface soil moisture content. Due to geographical variations in temperature and relative humidity, the long-term minimum and maximum fuel moistures in each grid cell varied across CONUS. Therefore, per Jolly et al. (2019), fuel moistures in each grid cell were converted to percentiles based on the local climatology such that in each grid cell the 1st percentile defined 1% of the locally driest conditions and the 99*th* percentile defined 1% of the locally wettest conditions. Fuel moistures were assigned to AF pixels by spatially and temporally intersecting the AF products with the 4 km gridded climatology.

2.2. Analysis

Analysis of nighttime fire activity across CONUS was mainly based upon the MODIS Terra and Aqua observations. The use of VIIRS was rare and limited to assessing the MODIS detection performance (Section 2.2.2) and complimenting the MODIS nighttime trend analysis (Section 2.2.3). Unless specifically noted, the following methods describe the analysis of the MODIS Terra and Aqua AF products.

2.2.1. Spatiotemporal patterns of nighttime fire activity

Diurnal fire activity across CONUS and throughout the year was characterized by aggregating MODIS daytime and nighttime AF pixels at a variety of spatiotemporal scales. Aggregations of AF pixels were summarized by summing per-pixel values of FRP (ΣFRP, MW). Admittedly, summing radiant heat release rates has no physical interpretation. Rather, observations of FRP should be temporally integrated to yield fire radiative energy (FRE, MJ). However, without the ability to fully resolve the diurnal cycle, estimating FRE from polar-orbiting observations requires more innovative approaches (Boschetti and Roy, 2009; Vermote et al., 2009; Kumar et al., 2011). Here it is simply assumed that ΣFRP is proportional to FRE (Freeborn et al., 2011). On occasion ΣFRP was decomposed into AF pixel counts, C, and mean per-pixel FRP, $\overline{\text{FRP}}$, such that $\Sigma\text{FRP} = C \times \overline{\text{FRP}}$. Active fire pixel counts have been related to burned area (Giglio et al., 2006b) and therefore can be considered indicators of the broad areal extent of fire activity. In contrast, mean per-pixel values of FRP are better indicators of local fire behaviour characteristics at sub-pixel resolutions.

Two proportions are most often reported in this work: the nighttime proportion (ϕ_N) and the wildfire proportion (ϕ_W), both expressed as percentages. The former is the proportion of total ΣFRP detected at night, and the latter is the proportion of total ΣFRP detected inside wildfires. The daytime proportion (ϕ_D) and the "outside wildfire" or the "other" fire type proportion (ϕ_O) are defined as complementary percentages:

$$100\% = \phi_N + \phi_D \tag{1}$$

$$100\% = \phi_W + \phi_O \tag{2}$$

Low values of ϕ indicate little fire activity relative to the total. For example, $\phi_N < 50\%$ indicates that less ΣFRP was detected at night compared to the day, and $\phi_W < 50\%$ indicates that less ΣFRP was detected inside wildfires compared to outside.

Nighttime and daytime proportions were partitioned into contributions from inside and outside wildfires, and ϕ_W and ϕ_O were partitioned into daytime and nighttime contributions. A deliberate notation is used to express these tiered proportions: the subscript identifies the secondary proportion (i.e., the child) and the superscript identifies the aggregation of AF pixels (i.e., the parent) from which the secondary proportion was calculated. Each parent was re-scaled so that the children added up to 100%. For example, the wildfire proportion at night is expressed as ϕ_W^N and the nighttime proportion inside wildfires is expressed as ϕ_N^W, which when added to their complements leads to the following:

$$100\% = \phi_W^N + \phi_O^N \tag{3}$$

$$100\% = \phi_N^W + \phi_D^W \tag{4}$$

Fig. 1 illustrates the calculation and notation of the tiered proportions. Lastly, large wildfire proportions (ϕ_G^W) were calculated as the percentage of ΣFRP detected in NWCG size class G relative to the total ΣFRP detected inside all wildfires.

2.2.2. Fuel moisture, nighttime persistence and detection performance

Diurnal and seasonal differences between vegetation fire types were summarized based on the near-surface environmental conditions at the times and locations of the AF detections. Cumulative sums and distributions of per-pixel values of FRP were generated as functions of 1000-hr fuel moisture percentiles. Nighttime proportions, wildfire proportions, and large wildfire proportions were similarly summarized whence AF pixels were aggregated by fuel moisture.

Although in reality many vegetation fires continue burning through the night, areas of flaming and smoldering combustion may not be large enough or intense enough at night to be detected by a satellite sensor. In this work nighttime persistence has a specific definition: when locations with a daytime AF detection were detected again at night. For every 24-hr period between 2012 and 2019, the MODIS Terra, Aqua and VIIRS AF pixels were projected onto the 4 km gridMET domain to provide one daytime and one nighttime detection mask for each sensor. The MODIS Terra and Aqua daytime masks were intersected to yield a single daytime mask indicating the 4km grid cells where both MODIS daytime

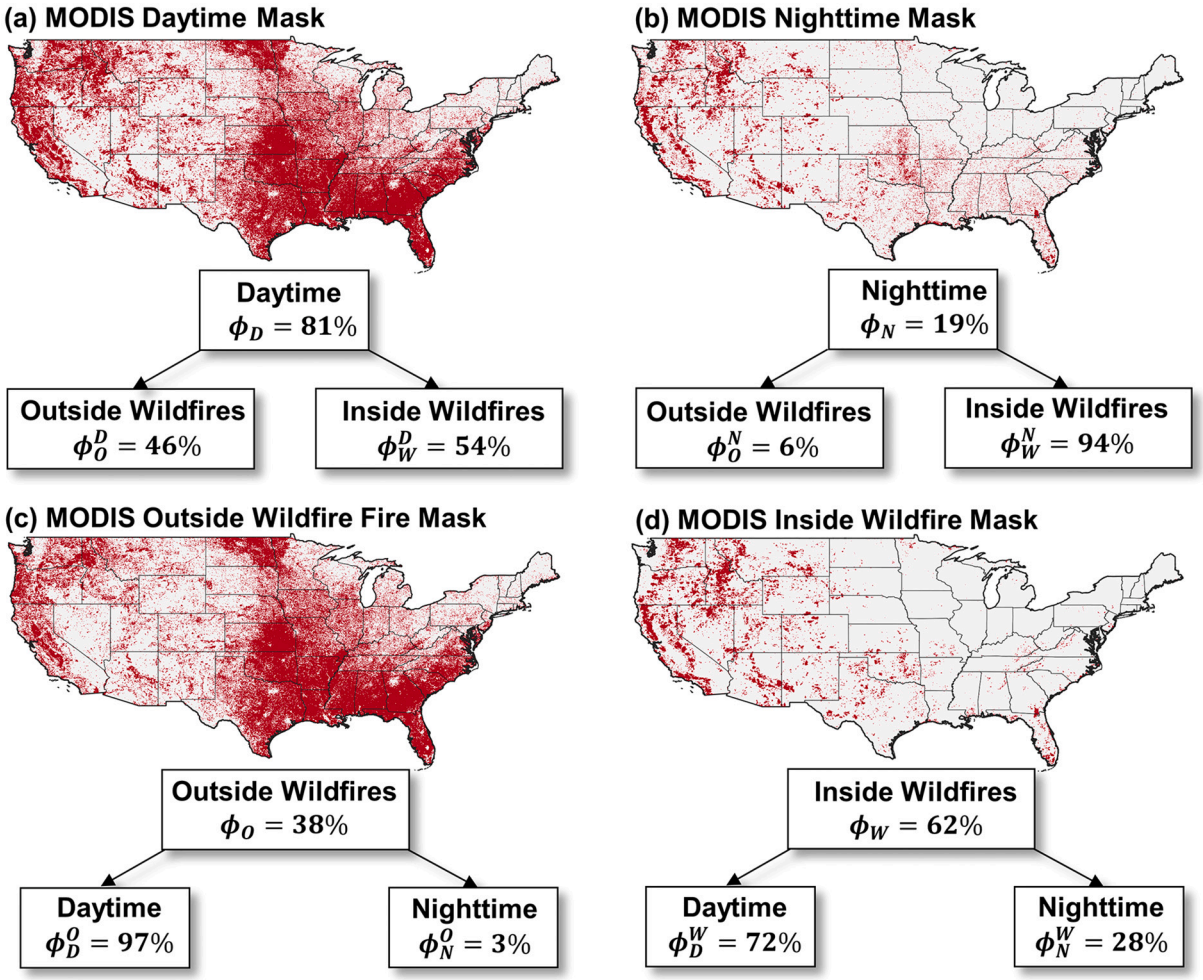

Fig. 1. Binary masks at 4 km grid cell resolution of locations across CONUS where from 2003 to 2020 MODIS detected at least one (a) daytime active fire (AF) pixel, (b) nighttime AF pixel, (c) AF pixel outside a wildfire, and (d) AF pixel inside a wildfire. Panels (a)–(d) also report proportions of the sum of fire radiative power detected during the day (ϕ_D), during the night (ϕ_N), outside wildfires (ϕ_O), and inside wildfires (ϕ_W), respectively. Daytime and nighttime proportions are decomposed into contributions from AF pixels detected outside and inside wildfires, and conversely, proportions outside and inside wildfires are decomposed into contributions from AF pixels detected during the daytime and nighttime.

overpasses detected an AF pixel. The MODIS daytime mask was then used to extract 1000-hr fuel moistures. Two separate nighttime masks were created for each 24-hr period: one for MODIS indicating the 4 km grid cells where either the Terra or Aqua nighttime overpass detected an AF pixel, and one for VIIRS. Nighttime masks were clipped to only those 4 km grid cells containing a MODIS daytime detection. This resulted in two datasets, one for MODIS and one for VIIRS, each consisting of 1000-hr fuel moistures and a binary response variable indicating whether daytime fire activity was detected again at night (i.e., "1") or not (i.e., "0"). All masks generated for each 24-hr period between 2012 and 2019 were accumulated. Using 1000-hr fuel moistures as the single explanatory variable, the probability of nighttime persistence was modelled separately for MODIS and VIIRS using logistic regressions fit to AF pixels detected inside wildfires, outside wildfires and for all AF pixels detected regardless of vegetation fire type.

To properly interpret MODIS observations of fire activity requires an understanding of the MODIS low spatial resolution detection bias, or the inability of MODIS to detect smaller, lower intensity vegetation fires (Freeborn et al., 2011). The MODIS daytime and nighttime detection performance was evaluated relative to the VIIRS daytime and nighttime AF detections, respectively, using the same set of masks constructed for the analysis of nighttime persistence. Since the MODIS Aqua overpass schedule more closely aligns with that of VIIRS, only the MODIS Aqua daytime and nighttime masks were utilized to ensure more direct comparisons. MODIS Aqua daytime and nighttime masks were clipped to those 4 km grid cells containing a VIIRS daytime or nighttime AF pixel, respectively. This resulted in two datasets, one for the daytime and one for the nighttime, consisting of 1000-hr fuel moistures and a binary response variable indicating the 4 km grid cells where MODIS Aqua failed to detect an AF pixel coincident with VIIRS (i.e., "1") or where MODIS Aqua successfully detected an AF pixel coincident with VIIRS (i.e., "0"). After all masks were accumulated over 8 yrs, the MODIS Aqua daytime and nighttime omission rates were modelled as functions of 1000-hr fuel moistures using logistic regressions fit to AF pixels detected inside wildfires, outside wildfires and for all AF pixels detected regardless of vegetation fire type.

The MODIS low spatial resolution detection bias is further complicated by increased pixel sizes at higher scan angles. The MODIS minimum detection threshold increases approximately 10-fold as a function of scan angle (Freeborn et al., 2011). Therefore, although smaller and/or lower intensity fires may trigger the MODIS AF detection algorithm near-nadir where pixel sizes are finer, fires must be larger and/or more intense to be detected near the swath edges where pixel sizes are coarser. Consequently, the ability of MODIS to detect nighttime persistence at any single overpass will depend on the location of the fire within the MODIS nighttime swath. Here, however, nighttime persistence was evaluated using both the MODIS Terra and Aqua overpasses. Occasions when a fire may not have been detected at the edge of the Terra

nighttime swath will have another opportunity a few hours later to be detected during the Aqua nighttime overpass, and vice versa, ameliorating the impact of the scan angle associated with a single overpass. Whilst VIIRS only offers a single nighttime overpass, increases in pixel sizes in the along-scan direction are minimized using a data aggregation scheme (Schroeder et al., 2014) thereby mitigating the impact of scan angle on the evaluation of nighttime persistence. Moreover, whilst we cannot discount the possible impact of scan angle on an individual night, nighttime persistence was evaluated over multiple years and thousands of nighttime overpasses. As such, the effects of scan angle on the evaluation of nighttime persistence will further average out over time if MODIS observes ground locations uniformly across the swath. This assumption was examined by intersecting the MODIS daytime masks with the MOD11A1 (Terra) and MYD11A1 (Aqua) Version 6 Land Surface Temperature and Emissivity Daily Global 1km products (Wan et al., 2015). Doing so enabled the retrieval of the nighttime scan angles at which MODIS detected - and more importantly - didn't detect nighttime persistence. Inspection confirmed that MODIS observed nighttime fire activity uniformly across the swath regardless of fire type or fuel moisture conditions, enabling MODIS nighttime persistence and omission rates to be interpreted without considering scan angle.

2.2.3. CONUS-wide trends

CONUS-wide trends from 2003 to 2020 were fit to the end-of-year wildfire statistics compiled by the National Interagency Coordination Center (NICC, 2021), which included annual burned area and annual wildfire counts from which annual mean wildfire sizes were calculated. Trends were fit to the NICC wildfire statistics since the MTBS and NIFS datasets did not contain a complete record of all wildfire occurrences or burned area. Nevertheless, to corroborate the perimeters used to identify AF pixels inside wildfires, annual burned areas were determined from the MTBS and NIFS datasets. CONUS-wide trends from 2003–2020 were fit to MODIS annual nighttime AF characteristics detected inside known wildfires. VIIRS annual nighttime AF characteristics inside known wildfires were also summarized between 2012 and 2020 for comparison, though trends were not fit to the VIIRS data due to the shortened time period. Since MODIS and VIIRS differ in spatial and temporal resolution, annual sums of nighttime FRP, annual nighttime AF pixel counts and annual nighttime mean per-pixel values of FRP from both sensors were normalized to standard anomalies (i.e., z-scores) based on the mean and standard deviations calculated from 2012 to 2020. Since large wildfire proportions, nighttime persistence and nighttime proportions for MODIS and VIIRS were calculated relative to each sensor they shared the same scale and did not require standardization. To avoid the influence of outliers, the slope and associated p-value of all trends were based on Thiel-Sen estimators.

Trends in nighttime wildfire activity observed by MODIS could be affected by two factors. First, due to the bow-tie-effect (Wolfe et al., 2002), MODIS pixels begin to overlap and may be double counted at high scan angles (Freeborn et al., 2014). Since pixels above 40° are affected by significant off-nadir bias (Giglio et al., 2006a), the fraction of AF pixels detected above this threshold, relative to the total annual count, was used quantify the possible impact of the bow-tie effect. The notion here is that if the relative contribution of AF pixels detected above 40° is constant, then the influence of double-counting at the swath edges can be discounted as a possible factor affecting the annual trends in nighttime fire activity. Secondly, nighttime cloud cover over wildfires could be decreasing, or increasing, providing satellite sensors with more, or less, opportunities to detect nighttime fire activity. To cope with this possibility, we utilized the MOD11A1 and MYD11A1 products to retrieve the nighttime land surface temperature (LST) at the locations where MODIS Terra and Aqua, respectively, detected daytime wildfire activity. Unless a clear-sky criteria is met, these products do not provide a nighttime LST, and the location with daytime wildfire activity is considered obscured at night. If the annual frequency of nighttime obscuration is constant, then the effects of cloud cover on the trends in nighttime wildfire activity can be discounted.

3. Results

3.1. Spatiotemporal patterns of nighttime fire activity

Between 2003 and 2020 MODIS detected approximately 1.9 million AF pixels across CONUS. Daytime AF pixels were widespread and accounted for 81% (i.e., $\phi_D = 81\%$) of the total ΣFRP detected by MODIS emitted from all vegetation fire types (Fig. 1a). Daytime fire activity detected by MODIS was nearly evenly split between inside and outside wildfires, with $\phi_W^D = 54\%$ and $\phi_O^D = 46\%$. In contrast, nighttime AF pixels were rarer and concentrated in western CONUS (Fig. 1b). Although MODIS nighttime AF pixels accounted for only 19% of the total ΣFRP detected over all vegetation fires ($\phi_N = 19\%$), the majority of nighttime ΣFRP was detected inside wildfires (i.e., $\phi_W^N = 94\%$). As such, the CONUS-wide MODIS nighttime proportion inside wildfires ($\phi_N^W = 28\%$, Fig. 1d) was considerably higher than for other vegetation fire types where very little fire activity located outside wildfires was detected during the night ($\phi_N^O = 3\%$, Fig. 1c).

Diurnal differences in MODIS AF detections varied spatially as evident from Fig. 1 which shows that localized nighttime proportions at 4 km resolution were zero across much of CONUS. Nighttime proportions outside wildfires were not investigated at a finer spatial scale, but nighttime proportions inside wildfires were determined for NWCG fire size classes (Fig. 2a). In general, nighttime proportions increased as AF pixels shifted from outside to inside wildfires and also with increasing wildfire size, ranging from a minimum of 7% in combined classes A and B to a maximum of 29% in class G. Nighttime AF detections in the largest wildfire size class G had the highest per-pixel values of FRP (Fig. 2b) and accounted for 95% of the nighttime ΣFRP detected in all wildfires. As such, wildfire size class G accounted for 89% of the nighttime ΣFRP detected by MODIS across CONUS regardless of vegetation fire type and therefore strongly influenced the overall nighttime proportion.

Interpreting the seasonality of CONUS-wide vegetation fire activity was complicated by the fact that monthly detections were composed of a variety of vegetation fire types and wildfire sizes burning in different locations. Nevertheless, in general, agricultural and prescribed fires prevailed across CONUS in the winter and spring while wildfires dominated in the summer and fall (Fig. 3a). Monthly CONUS-wide nighttime proportions varied through the year as the balance of AF pixels shifted into and out of wildfires such that ϕ_N was lowest during the winter and spring and highest during the summer and fall (Fig. 3b). Consequently the seasonality of ϕ_N and ϕ_W were well synchronized and strongly correlated at weekly resolution ($r^2 = 0.87$, $n = 52$).

3.2. Fuel moisture, nighttime persistence and detection performance

The seasonality of 1000-hr fuel moistures at the times and locations of MODIS AF detections coincided with the seasonality of wildfire activity such that fuel moistures were highest in the winter and spring and lowest in the summer and fall. MODIS detected half of the ΣFRP outside wildfires when 1000-hr fuel moistures were between the 12th and 51st percentiles. In contrast, MODIS detected half of the ΣFRP inside wildfires during much drier conditions, when 1000-hr fuel moistures were between the 1st and 7th percentiles. Although the fuel moisture distribution in all wildfires was heavily influenced by AF pixels detected in the largest size class G, MODIS was nevertheless capable of detecting smaller wildfires burning at higher fuel moistures (Fig. 4a). Therefore as fuel moistures decreased, not only did fire activity shift from outside to inside wildfires, as captured by the increasing wildfire proportion, ϕ_W, it also shifted from smaller to larger wildfires, as captured by the increasing large wildfire proportion, ϕ_G^W (Fig. 4b).

The CONUS-wide nighttime proportion, ϕ_N, also increased as 1000-

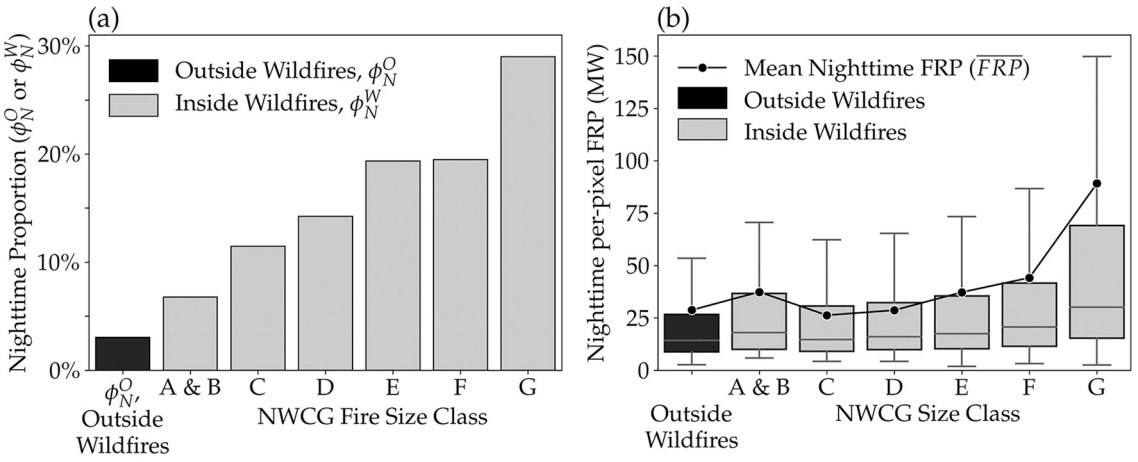

Fig. 2. (a) Nighttime proportions of the sum of fire radiative power (Σ*FRP*) detected by MODIS outside wildfires (ϕ_N^O) and inside wildfires (ϕ_N^W) sorted by fire size classes defined by the National Wildfire Coordinating Group, NWCG. (b) Nighttime per-pixel values of fire radiative power (FRP) detected by MODIS outside wildfires and inside wildfires sorted by NWCG size class. In (b), the boxes represent the interquartile range (IQR), the lower whiskers capture the minimum and the upper whiskers capture 1.5 × IQR, with outliers removed.

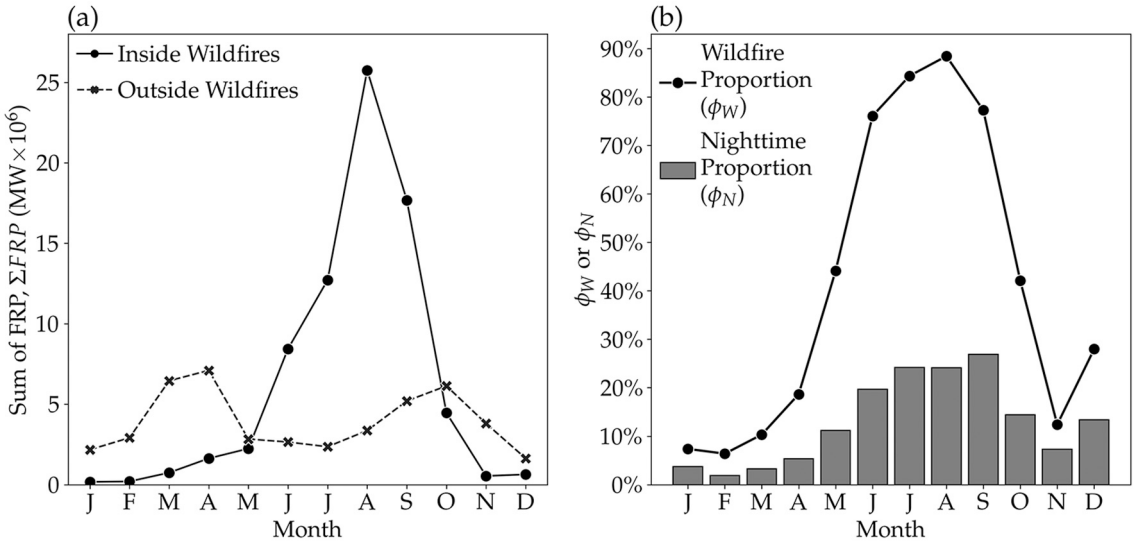

Fig. 3. (a) Monthly sums of fire radiative power (Σ*FRP*) detected by MODIS across CONUS from 2003–2020 separated by whether active fire pixels were located inside or outside wildfires. (b) Corresponding seasonal profiles of CONUS-wide wildfire proportions (ϕ_W) and nighttime proportions (ϕ_N).

hr fuel moistures decreased, particularly below the 50*th* percentile (Fig. 4b). The increase in ϕ_N with decreasing fuel moistures is partly attributed to a combination of and coupling between higher nighttime FRP values and greater nighttime persistence for larger wildfires. Due to lower per-pixel values of nighttime FRP, indicating smaller and lower intensity areas of combustion, MODIS was least likely to detect nighttime persistence outside of wildfires (Fig. 5a). Above the 50th percentile of 1000-hr fuel moistures when most AF pixels were detected outside wildfires, nearly all locations where Terra and Aqua detected daytime fire activity subsided by nightfall to drop below the MODIS minimum detection threshold. In contrast, with higher nighttime per-pixel values of FRP, MODIS was most capable of detecting nighttime persistence inside wildfires. As fuel moistures decreased and fire activity shifted into wildfires, AF pixels composed of larger and more intense areas of combustion were more readily distinguished from the non-fire background and the probability that MODIS detected nighttime persistence increased. Ultimately, the probability of MODIS detecting nighttime persistence achieved a maximum of 72% inside wildfires burning at the lowest fuel moistures, indicating that approximately three-quarters of 4 km grid cells that contained a MODIS Terra and Aqua daytime detection also contained either a MODIS Terra or Aqua nighttime detection.

Despite only providing a single nighttime observation, VIIRS with its finer spatial resolution was more capable of detecting nighttime persistence than MODIS (Fig. 5b). For CONUS, the MODIS minimum detection threshold at night was ~3 MW for AF pixels with a detection confidence of at least 50%. Based on the lowest 0.1% of per-pixel FRP values, the VIIRS minimum detection threshold at night was ~1 MW. The regions above the MODIS curves in Fig. 5a but below the VIIRS curves in Fig. 5b illustrate the MODIS low spatial resolution detection bias for different vegetation fire types. Vegetation fires within these regions continued burning into the night with sufficient size and intensity to trigger the VIIRS nighttime detection algorithm but were incapable of triggering the MODIS nighttime detection algorithm. Hence the nighttime Σ*FRP* emitted by vegetation fires burning within these regions was truncated by MODIS due to the omission of AF pixels containing smaller areas of lower intensity combustion burning below the MODIS ~3 MW nighttime detection threshold.

Without the ability to estimate the amount of nighttime Σ*FRP*

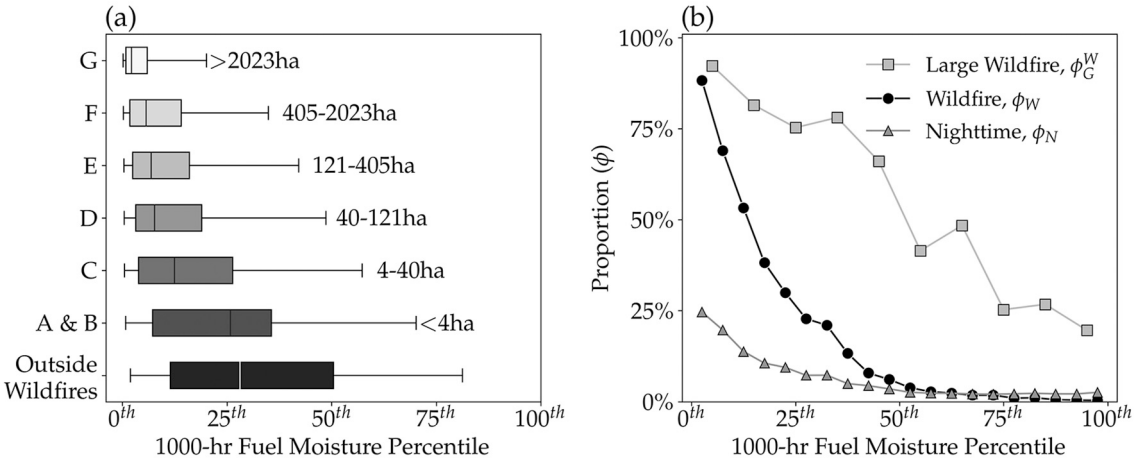

Fig. 4. (a) CONUS-wide cumulative distributions of the sum of fire radiative power (ΣFRP) detected by MODIS as a function of 1000-hr fuel moisture percentiles, grouped by whether active fire pixels were detected outside or inside wildfires sorted by size class. The whiskers indicate the range of fuel moistures over which MODIS detected 95% of the ΣFRP, the box captures the interquartile range, and the median line indicates the fuel moisture above and below which MODIS detected half of the ΣFRP in each group. (b) CONUS-wide nighttime proportions (ϕ_N), wildfire proportions (ϕ_W) and large wildfire proportions (ϕ_G^W) as a function of 1000-hr fuel moisture percentiles.

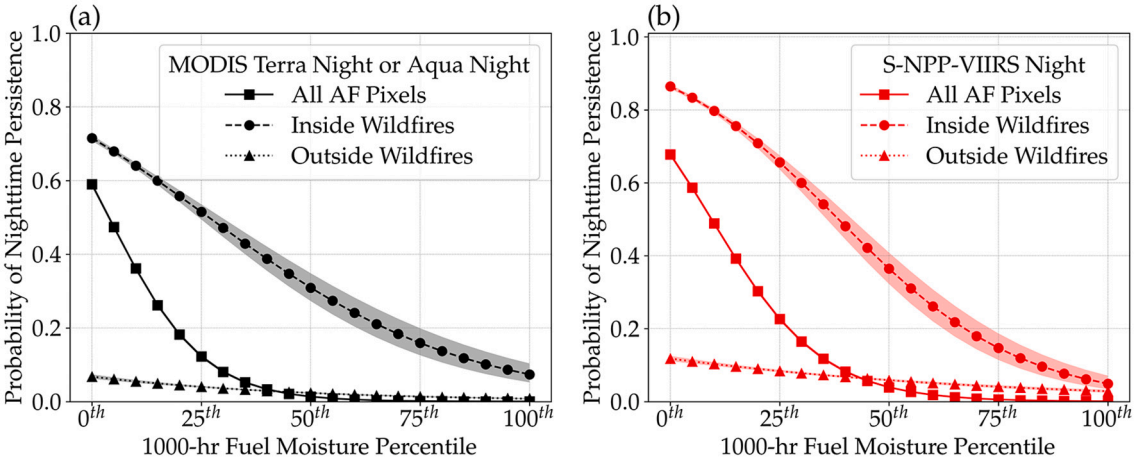

Fig. 5. Probability of (a) MODIS and (b) VIIRS detecting nighttime persistence as a function of 1000-hr fuel moisture percentiles. Given that both MODIS Terra and Aqua detected a daytime active fire (AF) pixel in a 4 km grid cell, the logistic regressions indicate the probability of (a) MODIS Terra or Aqua detecting a nighttime AF pixel in the same grid cell or (b) S-NPP VIIRS detecting a nighttime AF pixel in the same grid cell. Logistic regressions were built from AF pixels detected inside wildfires, outside wildfires and all AF pixels detected regardless of vegetation fire type. The shaded areas capture the 95% confidence interval of the logistic regression.

truncated by MODIS due to the low spatial resolution detection bias, the MODIS Aqua nighttime omission rate was used as a proxy. Compared to VIIRS, the nighttime detection performance of MODIS Aqua was poorest outside wildfires burning at the highest fuel moistures (Fig. 6a). Above the 50th percentile of 1000-hr fuel moistures, MODIS Aqua failed to detect more than 97% of the locations outside wildfires where VIIRS detected nighttime fire activity. Although the ability of MODIS Aqua to detect nighttime fire activity outside wildfires improved slightly over the full range of 1000-hr fuel moistures, the omission rate never dropped below 0.80. In contrast, MODIS Aqua was exceedingly more capable of detecting wildfires burning at night. Moreover, detection performance improved as fuel moistures decreased and fires became larger and more intense such that at the lowest 1000-hr fuel moistures the MODIS Aqua nighttime omission rate inside wildfires dropped to 0.59. MODIS Aqua performed best, however, when observing wildfires burning during the daytime (Fig. 6b). Although the MODIS Aqua daytime omission rate also decreased as 1000-hr fuel moistures decreased, the daytime detection performance curve was not parallel with the nighttime detection performance curve. Over the full range of 1000-hr fuel moistures, improvements in the MODIS Aqua nighttime omission rate were relatively greater than improvements in the MODIS Aqua daytime omission rate. Whereas from the highest to lowest fuel moistures, the MODIS Aqua nighttime omission rate inside wildfires dropped from 0.82 to 0.59, the MODIS Aqua daytime omission rate inside wildfires dropped from 0.31 to 0.17 (Fig. 6b). Hence higher MODIS nighttime proportions, ϕ_N, at lower fuel moistures (Fig. 4b) are at least partially attributed to a non-constant relationship between MODIS daytime and nighttime detection biases as fires grow larger.

3.3. CONUS-wide trends

During the MODIS era from 2003–2020, the NICC reported a significant ($p = 0.03$) positive trend of +0.05 Mha/yr in the annual area burned by wildfires across CONUS, which tracked well with estimates determined from the MTBS and NIFS perimeters used to identify AF pixels inside wildfires (Fig. 7a). The increase in burned area was not due

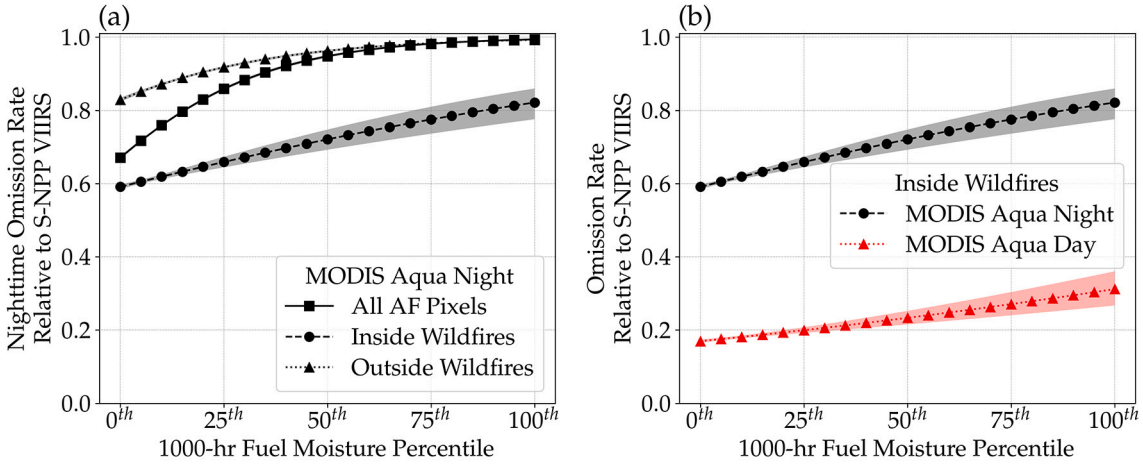

Fig. 6. Assessment of MODIS Aqua omission rates relative to VIIRS as functions of 1000-hr fuel moisture percentiles. A MODIS omission error is classified as a 4 km grid cell where VIIRS detected an active fire pixel (AF) but MODIS Aqua did not. Nighttime omission rates in (a) were based on logistic regressions built from AF pixels detected inside wildfires, outside wildfires and all AF pixels detected regardless of vegetation fire type. Nighttime and daytime omission rates shown for comparison in (b) were based on logistic regressions built from AF pixels detected inside wildfires only. The shaded areas capture the 95% confidence interval of the prediction.

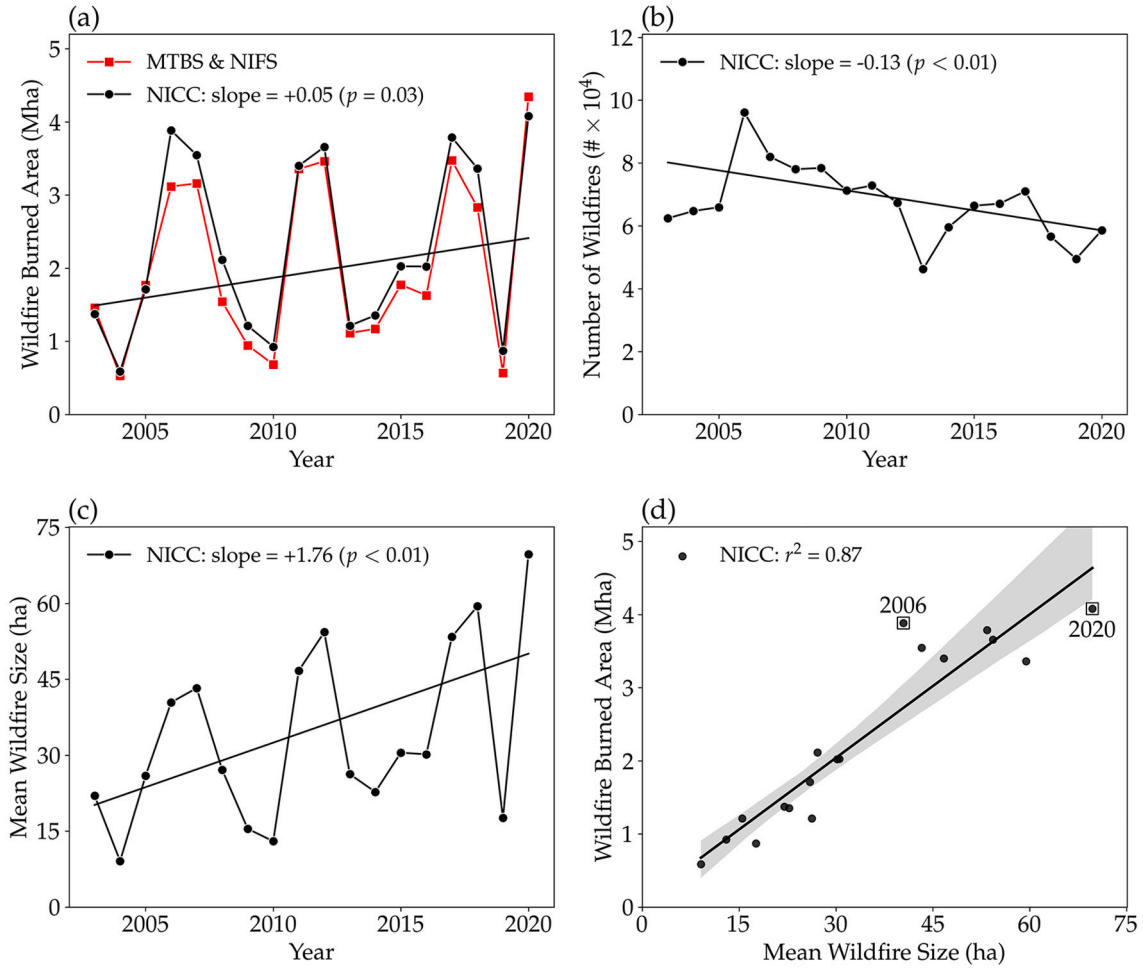

Fig. 7. Annual time-series of year-end CONUS-wide wildfire statistics compiled by the National Interagency Coordination Center (NICC, 2021). Also included for comparison are annual burned area estimates obtained from the Monitoring Trends in Burned Severity (MTBS) and National Incident Feature Service (NIFS) perimeters used to identify active fire pixels inside wildfires. The annual area burned by wildfires (a) and the annual number of wildfires reported by NICC (b) were used to calculate annual mean wildfire sizes (c). Trends based on Thiel-Sen estimates (with p-values) are shown in (a)–(c). The correlation between the annual area burned by wildfires and annual mean wildfire size is shown in (d).

to the number of wildfires, which actually declined (Fig. 7b), but rather due to an increase in the mean wildfire size (Fig. 7c), with mean wildfire sizes increasing by 32.3% during the latter 9 years of the study period (Table 1). Compared to the inverse relationship and poor correlation between annual burned area and the annual number of wildfires ($r^2 = 0.15$), annual burned area was positively and strongly correlated ($r^2 = 0.87$) with annual mean wildfire size (Fig. 7d). Two years in the study period illustrate two different ways to achieve the same annual burned area: either through numerous small wildfires or fewer but larger wildfires. Although the annual area burned by wildfires was nearly equivalent in 2006 and 2020 (3.9 and 4.1 Mha, respectively), the wildfire size distributions were different. Mean wildfire sizes in 2006 and 2020 were 40.4 and 69.7 ha, respectively, indicating that the area burned in 2020 was due to larger wildfires.

Based on annual z-scores, MODIS detected a significant ($p < 0.01$) positive trend in nighttime fire activity inside wildfires, with the latter 9 years showing good agreement with VIIRS. The positive trend in MODIS nighttime Σ*FRP* (Fig. 8a) is attributed to positive trends in both the annual AF pixel counts (Fig. 8b) as well as the annual mean nighttime FRP per-pixel, $\overline{\text{FRP}}$ (Fig. 8c). For reference, compared to 2003-2011, these three nighttime AF characteristics increased by 54%, 42% and 21%, respectively, over the latter half of the study period (Table 1). Moreover, despite the nearly equivalent areas burned by wildfires, the annual nighttime Σ*FRP* was 3.8× higher, the annual number of nighttime AF pixels was 2.5× higher, and the annual nighttime $\overline{\text{FRP}}$ was 1.5× higher in 2020 compared to 2006, demonstrating the influence of wildfire size distributions on retrievals of nighttime active fire characteristics. Since 2003, nighttime persistence has been more readily detected by MODIS (Fig. 8d and Table 1), indicating that locations with MODIS daytime AF pixels inside wildfires are becoming increasingly more likely of being detected again at night due to increased fire size and intensity, as evidenced by the increasing nighttime mean per-pixel FRP (Fig. 8c).

Although trends in the nighttime Σ*FRP* and AF pixel counts could be partially attributable to the bow-tie effect, whereby doublets of AF pixels were increasingly being detected at the swath edges, this artifact would be less likely to affect nighttime $\overline{\text{FRP}}$, nighttime persistence or the VIIRS observations. Nevertheless, an examination of the bow-tie effect revealed no significant trend ($p < 0.01$) in the relative contribution of AF pixels detected at scan angles greater than 40° to the total annual values. A change in the rate at which wildfire activity was obscured at night would have a broader impact, affecting all trends with the exception of the nighttime $\overline{\text{FRP}}$. However, based on the nighttime LST retrievals at the locations where MODIS detected daytime AF pixels, there was a slight, though significant ($p = 0.02$), increase in the nighttime obscuration of wildfires, perhaps due to increased nighttime smoke production. If increasing nighttime obscuration had any effect at all, it would have prevented the detection of nighttime fire activity.

Given that 95% of all MODIS nighttime Σ*FRP* detected inside wildfires was emitted from NWCG size class G, MODIS trends in nighttime fire activity inside wildfires were primarily driven by the largest wildfires. As corroborated by annual mean wildfire sizes, annual large wildfire proportions increased at a rate of +0.7% per year (Fig. 9a). Ultimately with a shift towards larger wildfires accompanied by increased nighttime per-pixel values of FRP and nighttime persistence, MODIS detected a significant ($p < 0.01$) positive trend in the annual nighttime proportion inside wildfires (Fig. 9b), suggesting that from 2003 to 2020 the rate of increase in nighttime fire activity outpaced the daytime. Although relative changes in MODIS active fire characteristics from the first half to the second half of the study period were greater for the nighttime compared to the daytime (Table 1), these comparisons inherently contain artifacts of the MODIS low spatial resolution detection bias. As such, correctly interpreting diurnal differences in the relative changes presented (Table 1) heavily relies on the assumption of a constant relationship between the MODIS daytime and nighttime omission rates over the full range of wildfire sizes (Fig. 6b).

Table 1
Wildfire statistics reported by the National Interagency Coordination Center (NICC, 2021) and MODIS daytime and nighttime active fire characteristics inside wildfires. All variables are summarized by the mean annual values observed in the first (2003–2011) and second (2012–2020) halves of the study period along with the relative change between halves.

	Mean		
	2003–2011	2012–2020	Relative change
Wildfire burned area (Mha)	2.1	2.5	+16.2%
Wildfire counts (# $\times 10^4$)	7.5	6.0	-23.9%
Mean wildfire size (ha)	27.9	41.3	+32.3%
Σ*FRP* (MW $\times 10^6$)			
Daytime	21.1	32.9	+35.6%
Nighttime	6.6	14.5	+54.3%
AF pixel counts (# $\times 10^4$)			
Daytime	12.6	18.2	+30.9%
Nighttime	9.3	16.0	+42.2%
$\overline{\text{FRP}}$ (MW)			
Daytime	168.1	180.3	+6.8%
Nighttime	71.6	90.6	+20.9%
Nighttime persistence	0.58	0.68	+15.6%
Large wildfire proportion (ϕ_G^W)	82.5%	91.2%	+10.6%
Nighttime proportion (ϕ_N^W)	23.8%	30.6%	+22.2%

4. Discussion

This work has revealed an active fire characteristic that can be used to help distinguish different vegetation fire types burning across CONUS. Similar to results found by Andela et al. (2015), compared to agricultural and prescribed fires, wildfires and particularly large wildfires are more likely to trigger the MODIS active fire detection algorithm at night. The ability of MODIS to detect vegetation fires is limited by the size and intensity of sub-pixel combustion areas (Wang et al., 2007). Agricultural and prescribed fire sizes are bounded by pre-planned fuel breaks designed to contain the fire, and their intensity is moderated by the decision to burn during low to moderate fire weather conditions (Knapp et al., 2009; Hiers et al., 2020). As fuels dry out and fire danger increases, agricultural and prescribed fires may be restricted by local, state, and federal agencies to prevent intentional ignitions from escaping control and becoming unwanted wildfires (Yoder, 2008; Prestemon et al., 2013). The probability of new wildfires increases with fire danger (Andrews et al., 2003), and despite the placement of fuel treatments and fuel breaks to interrupt their growth (Finney, 2007; Cochrane et al., 2012; Agee et al., 2000), extreme wildfire behaviour during historically dry and windy conditions may override landscape-scale fuel continuity (Prichard et al., 2020) and reduce suppression effectiveness (Plucinski, 2019). Hence, wildfire sizes and intensities were considerably greater than for agricultural and prescribed fires and were therefore more likely to be detected by MODIS at night.

Differences in fire diurnal cycles between vegetation fire types and wildfire sizes were directly captured by the nighttime proportion, ϕ_N. From Fig. 1, MODIS detected daytime fire activity without nighttime fire activity in many locations across CONUS. Only for the smallest, least intense vegetation fires that burned during the day and completely extinguished at night can values of $\phi_N = 0$ be considered accurate. However, it was not uncommon for MODIS to detect individual, longer duration vegetation fires burning on several consecutive days without detecting a single nighttime AF pixel. Values of $\phi_N = 0$ for these events were underestimated since, although these vegetation fires burned through the night in reality, the true nighttime FRP was not included in the estimation of ϕ_N due to the omission of nighttime AF pixels. Given the greater likelihood of dropping below the minimum detection threshold at night, it is expected that MODIS nighttime proportions were systematically underestimated for aggregations of smaller, lower

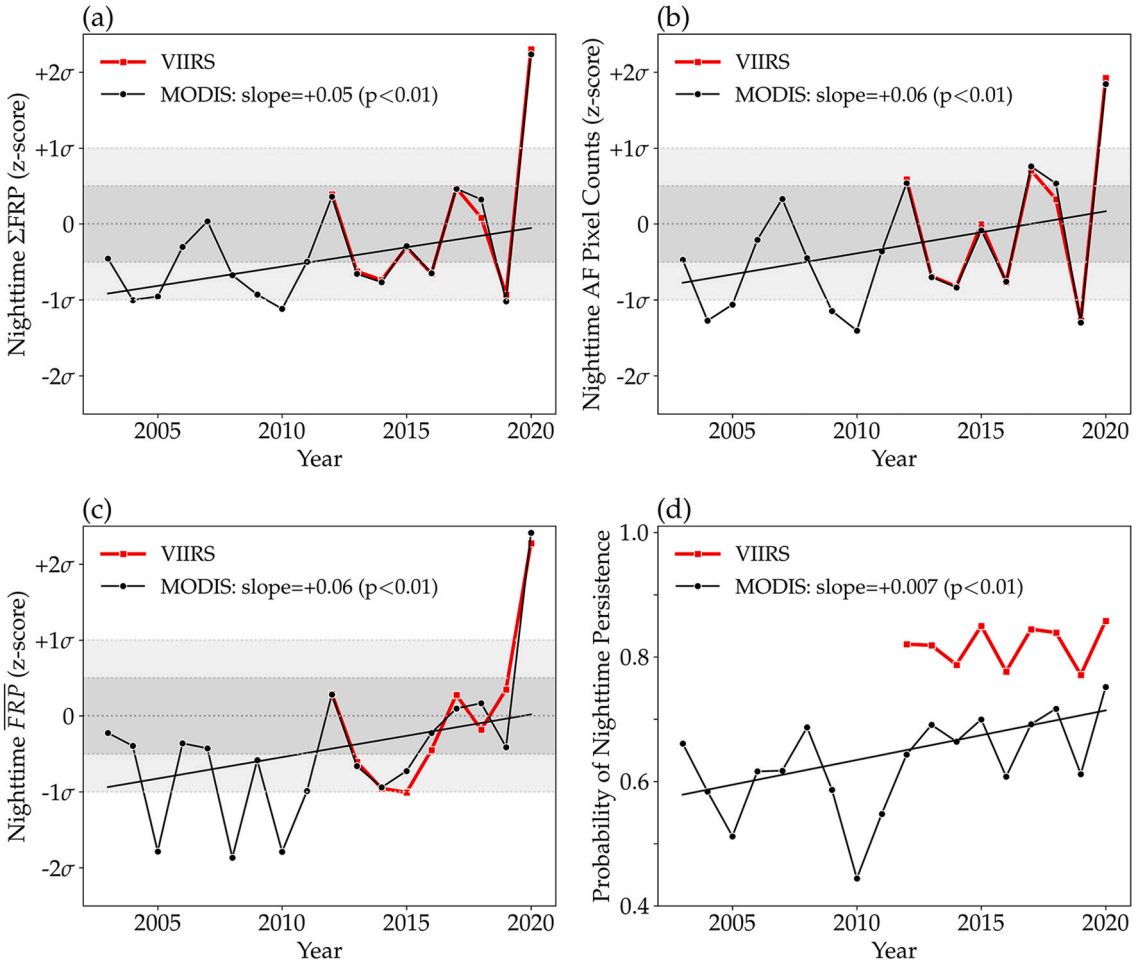

Fig. 8. CONUS-wide annual time-series of (a) sums of nighttime fire radiative power, Σ*FRP*, (b) nighttime active fire (AF) pixel counts, (c) nighttime mean FRP per pixel, $\overline{\text{FRP}}$, and (d) the probability of nighttime persistence. The MODIS (black) time series spans 2003–2020 and the VIIRS (red) time series spans 2012–2020. Nighttime AF characteristics in (a–c) are presented as standard anomalies (i.e., *z*-scores) to facilitate comparisons between MODIS and VIIRS. Thiel-Sen estimates (with *p*-values) are only shown for MODIS.

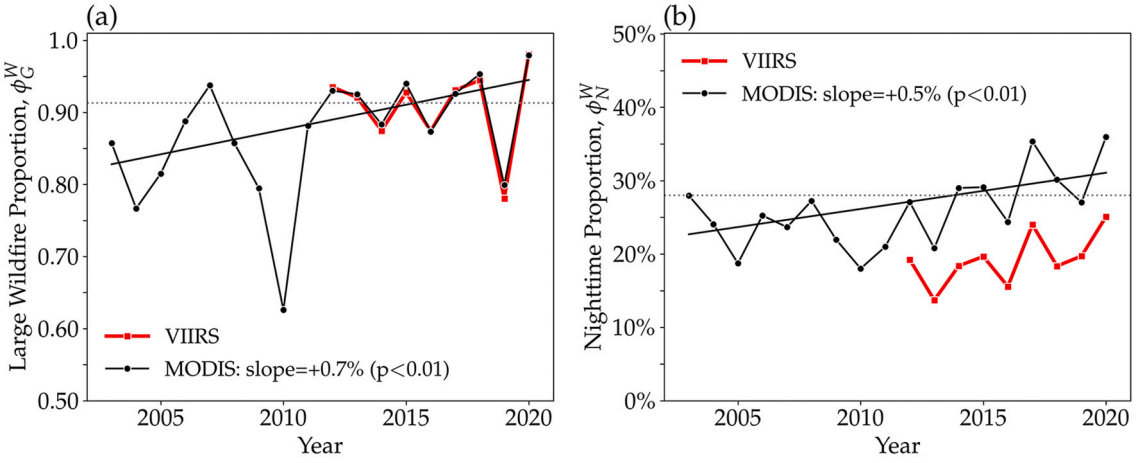

Fig. 9. CONUS-wide annual time-series of (a) large wildfire proportions, ϕ_G^W, and (b) nighttime proportions inside wildfires, ϕ_N^W, detected by MODIS and VIIRS. The MODIS (black) time series spans 2003–2020 and the VIIRS (red) time series spans 2012–2020. Thiel-Sen estimates (with *p*-values) are only shown for MODIS. The horizontal dotted lines at $\phi_G^W = 91\%$ and $\phi_N^W = 28\%$ indicates the CONUS-wide value detected by MODIS from 2003–2020.

intensity vegetation fires due to this low spatial resolution detection bias. Although nighttime proportions increased from a minimum of 3% for "other" fire types to a maximum of 29% for the largest wildfires (Fig. 2), it was not possible to quantify how much of this increase was attributed to reduced nighttime detection biases for larger fires or a genuine change in the shape of the fire diurnal cycles.

Based on empirical relationships with measurements of radiant heat release rates (Wooster et al., 2005; Freeborn et al., 2008), CONUS-wide trends in annual MODIS nighttime Σ*FRP* can be directly linked to increasing trends in nighttime fuel consumption and nighttime smoke production. Since it is often assumed that active fire pixel counts are proportional to burned area (Giglio et al., 2006b), the trend in nighttime AF pixel counts indicates an increase in the annual area burned by wildfires during the night, with the caveat that wildfire size distributions affect the MODIS nighttime detection performance. If the increase in annual burned area was driven by numerous small wildfires rather than fewer large fires, then it seems less likely that MODIS would have detected an increase in nighttime AF pixel counts, given that the ability of MODIS to detect nighttime persistence depends on fire size and intensity. At the local scale, an increase in mean nighttime per-pixel values of FRP indicates changes in nighttime fire behaviour characteristics. This could be attributed to either longer, deeper and more intense firelines during the night or larger pockets of more intense post-frontal combustion at night, both of which increase the difficulty of controlling a wildfire.

Interpreting the increasing trend in the nighttime proportion is confounded by the low spatial resolution detection bias. With a perfect sensor capable of detecting the true FRP, an increasing trend in the nighttime proportion would indicate that the rate of increase in nighttime fire activity is outpacing the increase in daytime fire activity. However both MODIS and VIIRS are imperfect sensors and fail to account for the FRP emitted from vegetation fires burning at night but below the minimum detection threshold. Hence the increasing trend in the nighttime proportion observed by MODIS is at least partially attributed to relatively better nighttime detection performance and thus a reduced truncation of nighttime FRP over larger, more intense vegetation fires. Although the MODIS low spatial resolution detection bias may seem like a disadvantage, it can nevertheless be used as a consistent threshold to gauge changes in vegetation fire activity. Ultimately, as mean wildfire sizes have increased across CONUS, nighttime fire activity has grown larger, more intense and therefore more capable of triggering the minimum detection threshold.

Increases in the annual area burned by wildfires and the frequency of large wildfires have been attributed to a variety of variables including temperature and vapor pressure deficit (Williams et al., 2014), within fire season precipitation (Holden et al., 2018), drought indicators (Riley et al., 2013), and fire danger indices (Barbero et al., 2014). The 1000-hr fuel moistures used herein were selected as a predictor variable since it is the major driver of the Energy Release Component, a common fire danger index produced by the US-based NFDRS. The 1000-hr fuel moistures were also selected because additional smaller size class fuels can easily be included to capture the influence of higher frequency fluctuations of fuel moistures on diurnal fire activity. Future work should incorporate 1-hr fuel moistures (Weise et al., 2005), which respond the quickest to changing atmospheric conditions, in order to capture the diurnal influences of the near-surface environment on relative changes in daytime and nighttime fire activity. Asymmetric changes in daytime and nighttime temperatures (Easterling et al., 1997; Davy et al., 2017) and/or vapor pressure deficit (Chiodi et al., 2021) may disproportionately affect nighttime fire activity more than the daytime and including 1-hr fuel moistures in the analysis may help confirm whether or not increases in nighttime wildfire activity across CONUS are truly outpacing the daytime.

5. Conclusion

In this study we have investigated the diurnal dynamics of active fire detections across the conterminous United States (CONUS) using nearly two decades of MODIS active fire data (2003–2020) stratified according vegetation fire type, wildfire size and time of detection (day/night). Whereas daytime fire activity was widespread, nighttime fire activity was concentrated inside wildfires, and particularly large wildfires in western CONUS. Analysis of coincident 1000-hr fuel moistures indicated that as fuels dried out, MODIS detected increasingly larger and more intense wildfires with higher probabilities of nighttime persistence and lower nighttime omission rates. Over the past 18 years, average wildfire sizes have increased across CONUS leading to both increases in daytime and nighttime MODIS active fire detections. Strictly interpreting the results without accounting for diurnal differences in the MODIS detection performance over larger wildfires suggests that increases in nighttime fire activity across CONUS have been outpacing the daytime. Increased nighttime fire activity has important implications for our ability to manage and contain wildfires and thus our ability to mitigate risks to firefighters and the public.

Declaration of Competing Interest

The authors declare that they have no known competing financial interests or personal relationships that could have appeared to influence the work reported in this paper.

Acknowledgments

The authors would like to thank the two anonymous reviewers and the editors for their comments and suggestions that helped improve this paper. M.A.C. participated in this work with support from NASA grant NNX11AB89G.

References

Abatzoglou, J.T., 2013. Development of gridded surface meteorological data for ecological applications and modelling. Int. J. Climatol. 33, 121–131. https://doi.org/10.1002/joc.3413.

Abt, K.L., Prestemon, J.P., Gebert, K.M., 2009. Wildfire suppression cost forecasts for the us forest service. J. Forestry 107, 173–178. https://doi.org/10.1093/jof/107.4.173.

Agee, J.K., Bahro, B., Finney, M.A., Omi, P.N., Sapsis, D.B., Skinner, C.N., van Wagtendonk, J.W., Weatherspoon, C.P., 2000. The use of shaded fuelbreaks in landscape fire management. Forest Ecol. Manag. 127, 55–66. https://doi.org/10.1016/S0378-1127(99)00116-4.

Aisbett, B., Wolkow, A., Sprajcer, M., Ferguson, S.A., 2012. "Awake, smoky, and hot": providing an evidence-base for managing the risks associated with occupational stressors encountered by wildland firefighters. Appl. Ergon. 43, 916–925. https://doi.org/10.1016/j.apergo.2011.12.013.

Andela, N., Kaiser, J., Van der Werf, G., Wooster, M., 2015. New fire diurnal cycle characterizations to improve fire radiative energy assessments made from MODIS observations. Atmos. Chem. Phys. 15, 8831–8846. https://doi.org/10.5194/acp-15-8831-2015.

Andrews, P.L., Loftsgaarden, D.O., Bradshaw, L.S., 2003. Evaluation of fire danger rating indexes using logistic regression and percentile analysis. IJWF 12, 213–226. https://doi.org/10.1071/WF02059.

Bagley, R.B., Clements, C.B., 2021. Extreme fire weather associated with nocturnal drying in elevated coastal terrain of California. Mon. Weather Rev. 149, 2497–2511. https://doi.org/10.1175/MWR-D-20-0241.1.

Barbero, R., Abatzoglou, J.T., Steel, E.A., Larkin, N.K., 2014. Modeling very large-fire occurrences over the continental United States from weather and climate forcing. Environ. Res. Lett. 9, 124009. https://doi.org/10.1088/1748-9326/9/12/124009.

Bhaduri, B., Bright, E., Coleman, P., Urban, M.L., 2007. Landscan USA: a high-resolution geospatial and temporal modeling approach for population distribution and dynamics. GeoJournal 69, 103–117. https://doi.org/10.1007/s10708-007-9105-9.

Boschetti, L., Roy, D.P., 2009. Strategies for the fusion of satellite fire radiative power with burned area data for fire radiative energy derivation. J. Geophys. Res.: Atmos. 114 (D20) https://doi.org/10.1029/2008JD011645.

Bowman, D., Balch, J.K., Artaxo, P., Bond, W.J., Carlson, J.M., Cochrane, M.A., D'Antonio, C.M., DeFries, R.S., Doyle, J.C., Harrison, S.P., Johnston, F.H., Keeley, J. E., Krawchuk, M.A., Kull, C.A., Marston, J.B., Moritz, M.A., Prentice, I.C., Roos, C.I., Scott, A.C., Swetnam, T.W., van der Werf, G.R., Pyne, S.J., 2009. Fire in the earth system. Science 324, 481–484. https://doi.org/10.1126/science.1163886.

Bradshaw, L.S., Deeming, J.E., Burgan, R.E., Cohen, J.D., 1984. The 1978 National Fire-Danger Rating System: Technical Documentation. General Technical Report INT-169. U.S. Department of Agriculture, Forest Service, Intermountain Forest and Range Experiment Station, Ogden, UT. https://doi.org/10.2737/INT-GTR-169, 44 p.

Britton, C., Lynch, C.F., Ramirez, M., Torner, J., Buresh, C., Peek-Asa, C., 2013. Epidemiology of injuries to wildland firefighters. Am. J. Emerg. Med. 31, 339–345. https://doi.org/10.1016/j.ajem.2012.08.032.

Chiodi, A.M., Potter, B.E., Larkin, N.K., 2021. Multi-decadal change in western US nighttime vapor pressure deficit. Geophys. Res. Lett. 48 https://doi.org/10.1029/2021GL092830 e2021GL092830.

Chuvieco, E., Aguado, I., Dimitrakopoulos, A.P., 2004. Conversion of fuel moisture content values to ignition potential for integrated fire danger assessment. Can. J. Forest Res. 34, 2284–2293. https://doi.org/10.1139/x04-101.
Cochrane, M.A., Moran, C.J., Wimberly, M.C., Baer, A.D., Finney, M.A., Beckendorf, K.L., Eidenshink, J., Zhu, Z., 2012. Estimation of wildfire size and risk changes due to fuels treatments. IJWF 21, 357–367. https://doi.org/10.1071/WF11079.
Cohen, J.D., Deeming, J.E., 1985. The National Fire-Danger Rating System: Basic Equations. Gen. Tech. Rep. PSW-GTR-82. U.S. Department of Agriculture, Forest Service, Pacific Southwest Forest and Range Experiment Station, Berkeley, CA. https://doi.org/10.2737/PSW-GTR-82, 16 p.
Cova, T.J., 2005. Public safety in the urban-wildland interface: should fire-prone communities have a maximum occupancy? Nat. Hazards Rev. 6, 99–108. https://doi.org/10.1061/(ASCE)1527-6988(2005)6:3(99.
Davies, D.K., Ilavajhala, S., Wong, M.M., Justice, C.O., 2009. Fire information for resource management system: archiving and distributing MODIS active fire data. IEEE Trans. GeoSci. Rem. Sens. 47, 72–79. https://doi.org/10.1109/TGRS.2008.2002076.
Davy, R., Esau, I., Chernokulsky, A., Outten, S., Zilitinkevich, S., 2017. Diurnal asymmetry to the observed global warming. Int. J. Climatol. 37, 79–93. https://doi.org/10.1002/joc.4688.
Dennison, P.E., Brewer, S.C., Arnold, J.D., Moritz, M.A., 2014. Large wildfire trends in the Western United States, 1984–2011. Geophys. Res. Lett. 41, 2928–2933. https://doi.org/10.1002/2014GL059576.
Dunn, C.J., O'Connor, C.D., Reilly, M.J., Calkin, D.E., Thompson, M.P., 2019. Spatial and temporal assessment of responder exposure to snag hazards in post-fire environments. Forest Ecol. Manag. 441, 202–214. https://doi.org/10.1016/j.foreco.2019.03.035.
Easterling, D.R., Horton, B., Jones, P.D., Peterson, T.C., Karl, T.R., Parker, D.E., Salinger, M.J., Razuvayev, V., Plummer, N., Jamason, P., Folland, C.K., 1997. Maximum and minimum temperature trends for the globe. Science 277, 364–367. https://doi.org/10.1126/science.277.5324.364.
Eidenshink, J., Schwind, B., Brewer, K., Zhu, Z.L., Quayle, B., Howard, S., 2007. A project for monitoring trends in burn severity. Fire Ecol. 3, 3–21. https://doi.org/10.4996/fireecology.0301003.
Finney, M.A., 2007. A computational method for optimising fuel treatment locations. IJWF 16, 702–711. https://doi.org/10.1071/wf06063.
Fosberg, M.A., Rothermel, R.C., Andrews, P.L., 1981. Moisture content calculations for 1000–hour timelag fuels. Forest Sci. 27, 19–26. https://doi.org/10.1093/forestscience/27.1.19.
Freeborn, P.H., Jolly, W.M., Cochrane, M.A., 2016. Impacts of changing fire weather conditions on reconstructed trends in US wildland fire activity from 1979 to 2014. J. Geophys. Res. BioSci. 121, 2856–2876. https://doi.org/10.1002/2016jg003617.
Freeborn, P.H., Wooster, M.J., Hao, W.M., Ryan, C.A., Nordgren, B.L., Baker, S.P., Ichoku, C., 2008. Relationships between energy release, fuel mass loss, and trace gas and aerosol emissions during laboratory biomass fires. J. Geophys. Res. Atmos. 113 https://doi.org/10.1029/2007jd008679.
Freeborn, P.H., Wooster, M.J., Roberts, G., 2011. Addressing the spatiotemporal sampling design of MODIS to provide estimates of the fire radiative energy emitted from Africa. Remote Sens. Environ. 115, 475–489. https://doi.org/10.1016/j.rse.2010.09.017.
Freeborn, P.H., Wooster, M.J., Roy, D.P., Cochrane, M.A., 2014. Quantification of MODIS fire radiative power (FRP) measurement uncertainty for use in satellite-based active fire characterization and biomass burning estimation. Geophys. Res. Lett. 41, 1988–1994. https://doi.org/10.1002/2013GL059086.
Giglio, L., Csiszar, I., Justice, C.O., 2006a. Global distribution and seasonality of active fires as observed with the terra and aqua moderate resolution imaging spectroradiometer (MODIS) sensors. J. Geophys. Res. Biogeosci. 111 https://doi.org/10.1029/2005JG000142.
Giglio, L., van der Werf, G.R., Randerson, J.T., Collatz, G.J., Kasibhatla, P., 2006b. Global estimation of burned area using MODIS active fire observations. Atmos. Chem. Phys. 6, 957–974. https://doi.org/10.5194/acp-6-957-2006.
Giglio, L., Schroeder, W., Justice, C.O., 2016. The collection 6 MODIS active fire detection algorithm and fire products. Remote Sens. Environ. 178, 31–41. https://doi.org/10.1016/j.rse.2016.02.054.
Gill, A.M., Stephens, S.L., Cary, G.J., 2013. The worldwide "wildfire" problem. Ecol. Appl. 23, 438–454. https://doi.org/10.1890/10-2213.1.
Graham, R.T., 2003. Hayman Fire Case Study. Gen. Tech. Rep. RMRS-GTR-114. U.S. Department of Agriculture, Forest Service, Rocky Mountain Research Station, Ogden, UT. https://doi.org/10.2737/RMRS-GTR-114, 396 p.
Hand, M., Katuwal, H., Calkin, D.E., Thompson, M.P., 2017. The influence of incident management teams on the deployment of wildfire suppression resources. IJWF 26, 615–629. https://doi.org/10.1071/wf16126.
Hiers, J.K., O'Brien, J.J., Varner, J.M., Butler, B.W., Dickinson, M., Furman, J., Gallagher, M., Godwin, D., Goodrick, S.L., Hood, S.M., Hudak, A., Kobziar, L.N., Linn, R., Loudermilk, E.L., McCaffrey, S., Robertson, K., Rowell, E.M., Skowronski, N., Watts, A.C., Yedinak, K.M., 2020. Prescribed fire science: the case for a refined research agenda. Fire Ecol. 16 https://doi.org/10.1186/s42408-020-0070-8.
Holden, Z.A., Swanson, A., Luce, C.H., Jolly, W.M., Maneta, M., Oyler, J.W., Warren, D. A., Parsons, R., Affleck, D., 2018. Decreasing fire season precipitation increased recent western US forest wildfire activity. Proc. Nat. Acad. Sci. 115, E8349–E8357. https://doi.org/10.1073/pnas.1802316115.
Jolly, W.M., Cochrane, M.A., Freeborn, P.H., Holden, Z.A., Brown, T.J., Williamson, G.J., Bowman, D., 2015. Climate-induced variations in global wildfire danger from 1979 to 2013. Nat. Commun. 6 https://doi.org/10.1038/ncomms8537.
Jolly, W.M., Freeborn, P.H., Page, W.G., Butler, B.W., 2019. Severe fire danger index: a forecastable metric to inform firefighter and community wildfire risk management. Fire 2, 47. https://doi.org/10.3390/fire2030047.
Knapp, E.E., Estes, B.L., Skinner, C.N., 2009. Ecological effects of prescribed fire season: a literature review and synthesis for managers. Gen. Tech. Rep. PSW-GTR-224. U.S. Department of Agriculture, Forest Service, Pacific Southwest Research Station, Albany, CA. https://doi.org/10.2737/PSW-GTR-224, 80 p.
Kuligowski, E.D., Walpole, E.H., Lovreglio, R., McCaffrey, S., 2020. Modelling evacuation decision-making in the 2016 Chimney Tops 2 fire in Gatlinburg, TN. IJWF 29, 1120–1132. https://doi.org/10.1071/wf20038.
Kumar, S.S., Roy, D.P., Boschetti, L., Kremens, R., 2011. Exploiting the power law distribution properties of satellite fire radiative power retrievals: a method to estimate fire radiative energy and biomass burned from sparse satellite observations. J. Geophys. Res. Atmos. 116 https://doi.org/10.1029/2011jd015676.
Larsen, B., Snow, R., Vincent, G., Tran, J., Wolkow, A., Aisbett, B., 2015. Multiple days of heat exposure on firefighters' work performance and physiology. PLoS One 10, e0136413. https://doi.org/10.1371/journal.pone.0136413.
Li, D.P., Cova, T.J., Dennison, P.E., Wan, N., Nguyen, Q.C., Siebeneck, L.K., 2019. Why do we need a national address point database to improve wildfire public safety in the US? Int. J. Disaster Risk Reduct. 39, 11. https://doi.org/10.1016/j.ijdrr.2019.101237.
Lin, H.W., McCarty, J.L., Wang, D., Rogers, B.M., Morton, D.C., Collatz, G.J., Jin, Y., Randerson, J.T., 2014. Management and climate contributions to satellite-derived active fire trends in the contiguous United States. J. Geophys. Res. Biogeosci. 119, 645–660. https://doi.org/10.1002/2013JG002382.
Littell, J.S., McKenzie, D., Peterson, D.L., Westerling, A.L., 2009. Climate and wildfire area burned in Western U.S. ecoprovinces, 1916–2003. Ecol. Appl. 19, 1003–1021. https://doi.org/10.1890/07-1183.1.
Little, J.B., 2020. One Climate-Change Wildfire Risk Lurks in the Dark. Scientific American. Springer Nature. https://www.scientificamerican.com/article/one-climate-change-wildfire-risk-lurks-in-the-dark/. accessed = 10-18-2021.
Mangan, R., 2007. Wildland Firefighter Fatalities in the United States: 1990-2006. NWCG PMS 841. National Wildfire Coordinating Group, Safety and Health Working Team, National Interagency Fire Center, Boise, ID, 28 p. https://www.nwcg.gov/publications/841.
McCarty, J.L., Justice, C.O., Korontzi, S., 2007. Agricultural burning in the Southeastern United States detected by MODIS. Remote Sens. Environ. 108, 151–162. https://doi.org/10.1016/j.rse.2006.03.020.
McCarty, J.L., Korontzi, S., Justice, C.O., Loboda, T., 2009. The spatial and temporal distribution of crop residue burning in the contiguous United States. Sci. Total Environ. 407, 5701–5712. https://doi.org/10.1016/j.scitotenv.2009.07.009.
McNamara, M.L., Semmens, E.O., Gaskill, S., Palmer, C., Noonan, C.W., Ward, T.J., 2012. Base camp personnel exposure to particulate matter during wildland fire suppression activities. J. Occup. Eviron. Hyg. 9, 149–156. https://doi.org/10.1080/15459624.2011.652934.
Moritz, M.A., Batlloria, E., Bradstock, R.A., Gill, A.M., Handmer, J., Hessburg, P.F., Leonard, J., McCaffrey, S., Odion, D.C., Schoennagel, T., Syphard, A.D., 2014. Learning to coexist with wildfire. Nature 515 (7525), 58–66. https://doi.org/10.1038/nature13946.
NICC, 2021. National Interagency Coordination Center, Wildland Fire Summary and Statistics Annual Reports. https://www.nifc.gov/fire-information/statistics. . accessed = 10-18-2021.
NIFS, 2021. National Incident Feature Services. https://www.nwcg.gov/publications/pms936/nifs. . accessed = 10-18-2021.
NWCG, 2021. National Wildfire Coordinating Group, Standards for Geospatial Operations. PMS 936. https://www.nwcg.gov/publications/pms936-1; accessed = 10-18-2021.
Page, W.G., Freeborn, P.H., Butler, B.W., Jolly, W.M., 2019. A review of US wildland firefighter entrapments: trends, important environmental factors and research needs. IJWF 28, 551–569. https://doi.org/10.1071/wf19022.
Plucinski, M.P., 2019. Fighting flames and forging firelines: wildfire suppression effectiveness at the fire edge. Curr. Forestry Rep. 5, 1–19. https://doi.org/10.1007/s40725-019-00084-5.
Prestemon, J.P., Hawbaker, T.J., Bowden, M., Carpenter, J., Brooks, M.T., Abt, K.L., Sutphen, R., Scranton, S., 2013. Wildfire ignitions: a review of the science and recommendations for empirical modeling. Gen. Tech. Rep. SRS-GTR-171. USDA-Forest Service, Southern Research Station, Asheville, NC. https://doi.org/10.2737/SRS-GTR-171, 20 p.
Prichard, S.J., Povak, N.A., Kennedy, M.C., Peterson, D.W., 2020. Fuel treatment effectiveness in the context of landform, vegetation, and large, wind-driven wildfires. Ecol. Appl. 30, e02104 https://doi.org/10.1002/eap.2104.
Randerson, J., Chen, Y., van der Werf, G., Rogers, B., Morton, D., 2012. Global burned area and biomass burning emissions from small fires. J. Geophys. Res. Biogeosci. 117, G04012 https://doi.org/10.1029/2012JG002128.
Riley, K.L., Abatzoglou, J.T., Grenfell, I.C., Klene, A.E., Heinsch, F.A., 2013. The relationship of large fire occurrence with drought and fire danger indices in the western USA, 1984–2008: the role of temporal scale. IJWF 22, 894–909. https://doi.org/10.1071/WF12149.
Riley, K.L., Thompson, M.P., Scott, J.H., Gilbertson-Day, J.W., 2018. A model-based framework to evaluate alternative wildfire suppression strategies. Resources 7, 4. https://doi.org/10.3390/resources7010004.
Roberts, G., Wooster, M., 2021. Global impact of landscape fire emissions on surface level PM2.5 concentrations, air quality exposure and population mortality. Atmos. Environ. 252, 118210. https://doi.org/10.1016/j.atmosenv.2021.118210.
Rossa, C.G., 2017. The effect of fuel moisture content on the spread rate of forest fires in the absence of wind or slope. IJWF 26, 24–31. https://doi.org/10.1071/WF16049.

Ryan, K.C., Knapp, E.E., Varner, J.M., 2013. Prescribed fire in North American forests and woodlands: history, current practice, and challenges. Front. Ecol. Environ. 11, e15–e24. https://doi.org/10.1890/120329.

Schroeder, W., Oliva, P., Giglio, L., Csiszar, I.A., 2014. The new VIIRS 375 m active fire detection data product: algorithm description and initial assessment. Remote Sens. Environ. 143, 85–96. https://doi.org/10.1016/j.rse.2013.12.008.

Short, K.C., 2014. A spatial database of wildfires in the United States, 1992–2011. Earth Syst. Sci. Data 6, 1–27. https://doi.org/10.5194/essd-6-1-2014.

Stephens, S.L., 2005. Forest fire causes and extent on United States Forest Service lands. IJWF 14, 213–222. https://doi.org/10.1071/wf04006.

Stephens, S.L., McIver, J.D., Boerner, R.E., Fettig, C.J., Fontaine, J.B., Hartsough, B.R., Kennedy, P.L., Schwilk, D.W., 2012. The effects of forest fuel-reduction treatments in the United States. Bioscience 62, 549–560. https://doi.org/10.1525/bio.2012.62.6.6.

Syphard, A.D., Keeley, J.E., Bar Massada, A., Brennan, T.J., Radeloff, V.C., 2012. Housing arrangement and location determine the likelihood of housing loss due to wildfire. PLoS One 7, e33954. https://doi.org/10.1371/journal.pone.0033954.

Vermote, E., Ellicott, E., Dubovik, O., Lapyonok, T., Chin, M., Giglio, L., Roberts, G.J., 2009. An approach to estimate global biomass burning emissions of organic and black carbon from MODIS fire radiative power. J. Geophys. Res. Atmos. 114 https://doi.org/10.1029/2008JD011188.

Vincent, G.E., Aisbett, B., Wolkow, A., Jay, S.M., Ridgers, N.D., Ferguson, S.A., 2018. Sleep in wildland firefighters: what do we know and why does it matter? IJWF 27, 73–84. https://doi.org/10.1071/WF17109.

Viney, N.R., 1991. A review of fine fuel moisture modelling. IJWF 1, 215–234. https://doi.org/10.1071/WF9910215.

Wan, Z., Hook, S., Hulley, G., 2015. MOD11A1 MODIS/Terra Land Surface Temperature/Emissivity Daily L3 Global 1 km SIN Grid V006 [Data set]. NASA EOSDIS Land Processes DAAC. NASA. https://doi.org/10.5067/MODIS/MOD11A1.006 accessed = 10-18-2021.

Wang, W.T., Qu, J.J., Hao, X.J., Liu, Y.Q., Sommers, W.T., 2007. An improved algorithm for small and cool fire detection using MODIS data: a preliminary study in the Southeastern United States. Remote Sens. Environ. 108, 163–170. https://doi.org/10.1016/j.rse.2006.11.009.

Weise, D.R., Fujioka, F.M., Nelson, R.M., 2005. A comparison of three models of 1-h time lag fuel moisture in Hawaii. Agri. Forest Meteorol. 133, 28–39. https://doi.org/10.1016/j.agrformet.2005.03.012.

Westerling, A.L., Hidalgo, H.G., Cayan, D.R., Swetnam, T.W., 2006. Warming and earlier spring increase western US forest wildfire activity. Science 313, 940–943. https://doi.org/10.1126/science.1128834.

Williams, A.P., Seager, R., Berkelhammer, M., Macalady, A.K., Crimmins, M.A., Swetnam, T.W., Trugman, A.T., Buenning, N., Hryniw, N., McDowell, N.G., et al., 2014. Causes and implications of extreme atmospheric moisture demand during the record-breaking 2011 wildfire season in the Southwestern United States. J. Appl. Meteorol. Climatol. 53, 2671–2684. https://doi.org/10.1175/JAMC-D-14-0053.1.

Williamson, G.J., Prior, L.D., Jolly, W.M., Cochrane, M.A., Murphy, B.P., Bowman, D.M., 2016. Measurement of inter-and intra-annual variability of landscape fire activity at a continental scale: the Australian case. Environ. Res. Lett. 11, 035003. https://doi.org/10.1088/1748-9326/11/3/035003.

Withen, P., 2015. Climate change and wildland firefighter health and safety. New Sol.: J. Environ. Occup. Health Pol. 24, 577–584. https://doi.org/10.2190/NS.24.4.i.

Wolfe, R.E., Nishihama, M., Fleig, A.J., Kuyper, J.A., Roy, D.P., Storey, J.C., Patt, F.S., 2002. Achieving sub-pixel geolocation accuracy in support of MODIS land science. Remote Sens. Environ. 83, 31–49. https://doi.org/10.1016/S0034-4257(02)00085-8.

Wong, S.D., Chorus, C.G., Shaheen, S.A., Walker, J.L., 2020. A revealed preference methodology to evaluate regret minimization with challenging choice sets: a wildfire evacuation case study. Travel Behav. Soc. 20, 331–347. https://doi.org/10.1016/j.tbs.2020.04.003.

Wooster, M.J., Roberts, G., Perry, G.L.W., Kaufman, Y.J., 2005. Retrieval of biomass combustion rates and totals from fire radiative power observations: FRP derivation and calibration relationships between biomass consumption and fire radiative energy release. J. Geophys. Res. Atmos. 110 https://doi.org/10.1029/2005jd006318.

Yoder, J., 2008. Liability, regulation, and endogenous risk: the incidence and severity of escaped prescribed fires in the United States. J. Law Econ. 51, 297–325. https://doi.org/10.1086/589661.